Magnesium Modulates ROMK Channel–Mediated Potassium Secretion

Lei Yang, Gustavo Frindt, and Lawrence G. Palmer

Department of Physiology and Biophysics, Weill Medical College of Cornell University, New York, New York

ABSTRACT

The ability of intracellular and extracellular Mg^{2+} to block secretory K^+ currents through ROMK channels under physiologic conditions is incompletely understood. We expressed ROMK2 channels in *Xenopus* oocytes and measured unitary currents in the inside-out and cell-attached modes of the patch-clamp technique. With 110 mM K^+ on both sides of the membrane, 0.2 to 5 mM Mg^{2+} on the cytoplasmic side reduced outward currents, but not inward currents, at $V_m > 0$. With 11 or 1.1 mM extracellular K^+ ($[K^+]_o$), $\geq$0.2 mM Mg^{2+} blocked outward currents in the physiologic V_m range (0 to −60 mV). With decreasing $[K^+]_o$, the apparent dissociation constant of the blocker decreased, but the voltage dependence of block did not significantly change. Whole-cell recordings from principal cells of rat cortical collecting ducts revealed similar inhibitory effects of intracellular Mg^{2+}. Mg^{2+} added to the extracellular solution also reduced single-channel currents with an affinity that increased as $[K^+]_o$ decreased. In conclusion, physiologic concentrations of intracellular and extracellular Mg^{2+} can influence secretory K^+ currents through ROMK channels. These effects could play a role in the modulation of K^+ transport under conditions of K^+ and/or Mg^{2+} depletion.

J Am Soc Nephrol 21: 2109–2116, 2010. doi: 10.1681/ASN.2010060617

Interactions between Mg^{2+} and K^+ cations can affect K homeostasis.[1–3] In particular, under conditions of Mg deficiency, it can be difficult to restore K balance unless the Mg deficit is corrected.[4] Recently, Huang and Kuo[5] suggested that Mg^{2+} block of rat outer medullary K (ROMK) or Kir1.1 channels might play a role in this phenomenon.

Experiments with starfish eggs,[6] and cardiac myocytes,[7] first showed that intracellular Mg^{2+} can block K^+ channels in a voltage-dependent manner, accounting in part for the property of inward rectification. After the molecular identification and cloning of the inward-rectifier K channel family, it was shown that internal Mg^{2+} is a potent blocker of the so-called "strong" inward rectifiers, including those of the Kir2 and Kir3 families, but is much less effective on the "weak" inward rectifiers, such as Kir1 and Kir6. The differences are accounted for in part by critical negative charges in the transmembrane and cytoplasmic parts of the channels.[8–10]

A key aspect of the hypothesis of Huang and Kuo[5] was that the affinity of block by Mg^{2+} would be increased to levels comparable to physiologic concentrations when extracellular (luminal) K^+ was low. The dependence of the affinity of the blocking ions on extracellular permeant ions is a hallmark of strong inward rectifiers,[11–13] but relatively little information is available for weak rectifiers such as ROMK. Lu and MacKinnon[8] showed that decreasing external K^+ increased the blocking affinity of internal Mg^{2+} in ROMK but did not study K^+ concentrations below 40 mM.

In this paper, we test the affinity of block of ROMK channels by intracellular Mg^{2+} at different concentrations of extracellular K^+. We find that

Received June 11, 2010. Accepted August 11, 2010.

Published online ahead of print. Publication date available at www.jasn.org.

Correspondence: Dr. Lawrence G. Palmer, Department Physiology and Biophysics, Weill Medical College of Cornell University, 1300 York Avenue, New York, NY 10065. Phone: 212-746-6355; Fax: 212-746-8690; E-mail: lgpalm@med.cornell.edu

when extracellular K^+ is 1 to 10 mM, as expected for fluid entering the K^+-secretory part of the nephron, the channels are blocked by Mg^{2+} concentrations of 1 mM or less over the physiologic voltage range of the apical membrane. We also explored block of the channels by extracellular Mg^{2+}.

RESULTS

Figure 1 shows recordings from excised inside-out patches from an oocyte expressing ROMK2, with 110 mM K^+ on both sides of the membrane. In Figure 1A, the cytoplasmic (bath) solution contained no added Mg^{2+}. Figure 1B shows another patch under identical conditions except for the addition of 1 mM Mg^{2+} to the bath solution. In the absence of Mg^{2+}, inward and outward currents are comparable for the same electrical driving force, and the current-voltage (*I-V*) relationship is nearly linear over the voltage range of ±100 mV (Figure 1C), with only mild inward rectification. In the presence of Mg^{2+}, inward currents are affected very little, but outward currents decrease in a voltage-dependent manner. The results are similar to those reported previously.[8,14] Currents with lower (0.2 mM) and higher (5 mM) Mg^{2+} are also plotted in Figure 1C. Thus, under conditions of high K^+ in the lumen and negative membrane potentials, physiologic levels of intracellular Mg^{2+} (assumed to be <1 mM, see Discussion) will have little effect on currents through ROMK channels.

Figure 2 shows a situation in which conditions mimic more closely those that pertain to renal K^+ secretion in the distal nephron. Here the K^+ concentration in the extracellular (pipette) solution is reduced to 11 mM, allowing outward flow of K^+ for membrane voltages greater than −60 mV. Currents shown in Figure 2, A and B, were obtained with bath solutions identical to those in Figure 1. In the absence of Mg^{2+}, the *I-V* relationship shifts from inward to moderate outward rectification and the reversal potential shifts to approximately −60 mV, reflecting the change in the equilibrium potential for K^+. Again, outward currents are decreased in the presence of different concentrations of Mg^{2+} in the bath. However, in this case, the inhibition can be observed with negative membrane potentials.

Extracellular K^+ was further reduced to 1.1 mM, as shown in Figure 3. This concentration could pertain to renal tubular fluid as it enters the distal convoluted tubule.[15] Here inward currents could not be measured because the reversal potential was shifted to values less than −100 mV, as expected from the K^+ equilibrium potential. Outward currents at voltages greater than −50 mV were clearly inhibited by Mg^{2+}, even at low (0.2 mM) concentrations. As with the other external K^+ concentrations, the fractional inhibition of current was voltage dependent.

The voltage dependence of block was analyzed as described in the Concise Methods section (Figure 4). The value of the intrinsic K_i, $K_{i,Mg}(0)$, decreased as the external $[K^+]$ was lowered, with about a fourfold change from 110 to 1 mM. Values of the apparent valence ($z\delta$) were similar at 0.6 to 0.65 for all external K^+ concentrations (Table 1).

To confirm these results in a physiologically relevant cell, we carried out whole-cell clamp measurements in principal cells of the rat cortical collecting ducts (CCDs). Pipette solutions contained 140 mM K^+ with or without 1.2 mM Mg, and bath solutions contained 5 mM K^+. Kir1.1 activity was assessed as the outward current at a holding potential of 0 mV that was inhibited by the modified honey bee toxin Tertiapin-Q (TPNQ), termed I_{SK}, as described previously.[16] Examples of these currents are shown in Figure 5, A and B. There was considerable variability in the magnitude of this current from cell to cell and especially from tubule to tubule. To partially control for this variability, we made measurements with and without Mg^{2+} in paired cells from the same tubules. As shown in Figure 5C, mean values of I_{SK} in the presence of internal Mg^{2+} were 30% of

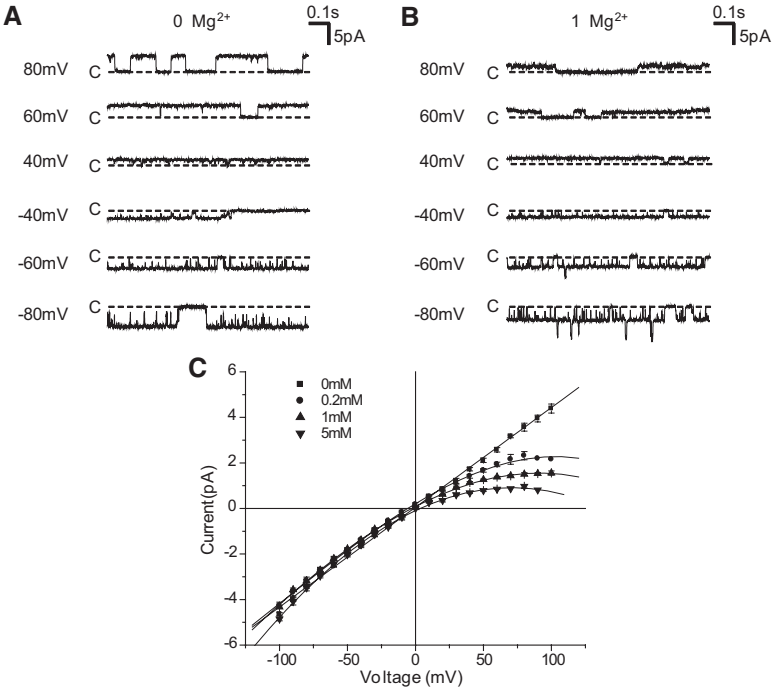

Figure 1. Intracellular Mg^{2+} blocks ROMK currents with 110 mM extracellular K^+. (A) Currents in an inside-out patch in the absence of Mg^{2+}. (B) Currents in an inside-out patch in the presence of 1 mM Mg^{2+}. Dashed lines indicate current levels when all channels are closed. (C) *I-V* relationships for 0, 0.2, 1, and 5 mM Mg^{2+}. At each voltage, current values represent means ± SEM for two to eight patches. Lines are smooth curves drawn through the points.

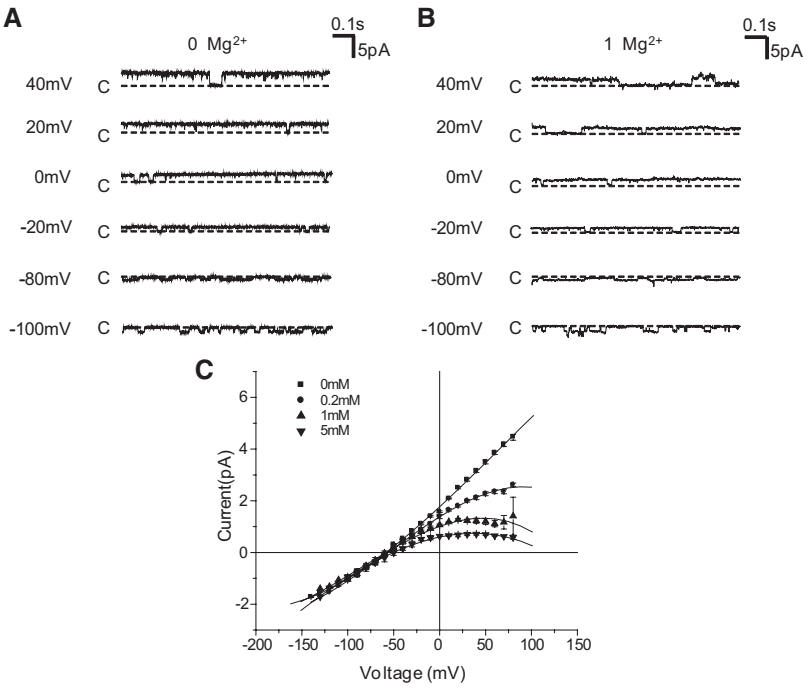

Figure 2. Intracellular Mg^{2+} blocks ROMK currents with 11 mM extracellular K^+. (A) Currents in an inside-out patch in the absence of Mg^{2+}. (B) Currents in an inside-out patch in the presence of 1 mM Mg^{2+}. Dashed lines indicate current levels when all channels are closed. (C) *I-V* relationships for 0, 0.2, 1, and 5 mM Mg^{2+}. At each voltage, current values represent means ± SEM for 2 to 12 patches. Lines are smooth curves drawn through the points.

that measured in cells in the absence of Mg^{2+}. Currents measured in the same tubule were highly correlated (Figure 5D). The mean ratio of current with and without Mg^{2+} was 0.31 ± 0.03. Also plotted in Figure 5C are results of similar experiments using animals fed a high-K diet for 1 week. Here, a similar degree of inhibition was observed, although in this case, the measurements were not paired. Because of the presence of large currents from basolateral K^+ and Cl^- channels, it was not possible to routinely establish the voltage dependence of the Mg^{2+}effect in the CCD.

Single-channel currents through ROMK channels in the CCD do exhibit rectification, consistent with block by Mg^{2+}. Figure 6 shows the *I-V* relationship in the cell-attached configuration with 140 mM K^+ in the pipette to match that in the cytoplasm. The data are well described by equations 1 and 2 using values of $K_i(0)$ and δ determined in oocytes and assuming cytoplasmic $[Mg^{2+}] = 0.7$ mM.

During periods of dietary Mg restriction and Mg deficiency, the concentration of the ion in the luminal fluid of the distal nephron will also decrease.[17,18] We therefore studied the effects of extracellular Mg^{2+} on ROMK channel currents. Figure 7 shows single-channel currents with either 0 (A) or 3 mM (B) Mg^{2+} in the pipette solution, along with 11 mM K. In this case, both the inward and the outward currents were reduced in the presence of extracellular Mg^{2+}, although inward currents were more affected. Smaller reductions were measured with 1 mM Mg^{2+} (Figure 7C). We used equations 1 and 2 to analyze these data as well, as shown in Figure 7D. Here the inhibition constants for external Mg^{2+} block in the absence of a voltage were larger (6 to 7 mM) than those for internal block (1 to 2 mM; Figure 4) under similar conditions (Table 2). The voltage dependence was reversed, as expected if Mg^{2+} binds within the electric field across the membrane. Block by external Mg^{2+} was also reduced by increased extracellular K^+; with 110 mM K^+ in the pipette solution, $K_i(0)$ increased to 19 mM (Figure 7D).

To assess the impact of Mg^{2+} block on K^+ secretion, we used a numerical model of the connecting tubule (CNT)/CCD used previously to study transepithelial K^+ transport.[16,19] Mg^{2+} block was incorporated into the model in the presence of low luminal K^+ by assuming two blocking sites, one for cytoplasmic Mg^{2+} with a $K_i(0)$ of 1.4 or 0.6 mM, corresponding to results from single-channel and whole-cell measurements, respectively, and a $z\delta$ value of 0.64, and a second site for luminal Mg^{2+} with a $K_i(0)$ of 6.2 mM and $z\delta$ value of 0.24. We further assumed that luminal and cytoplasmic Mg^{2+} would change in parallel. Varying Mg^{2+} from 0 to 1 mM reduced net secretory K^+ flux J_K (Figure 8A) and the apical K^+ conductance G_K (Figure 8B) by up to 55%, depending on the unblocked apical K^+ conductance. The larger percentage block at lower basal G_K reflects the depolarization of the apical membrane voltage. The relationship between the maximal block at 1 mM Mg^{2+} and the unblocked conductance is shown in Figure 8C.

DISCUSSION

We showed that intracellular Mg^{2+} can block ROMK channels under physiologic conditions, particularly those that would apply to the kidney during dietary K restriction. With high (100 mM) extracellular (luminal) K^+, Mg^{2+} blocked only outward currents at positive membrane potentials, in agreement with previous results.[8,14] We estimated the apparent K_i in the absence of a membrane potential $[K_i(0)]$ to be about 5 mM with a voltage dependence ($z\delta$) of approximately 0.6. Earlier studies reported a somewhat lower affinity [$K_i(0) \sim 13$ mM] and higher voltage dependence ($z\delta \sim 1$).[8] The difference may reflect different methods of measurement; we used single-channel events, whereas Lu and Mackinnon assessed macroscopic currents.[8] However, the differences do not affect the main conclusions of our study. The increase in the apparent

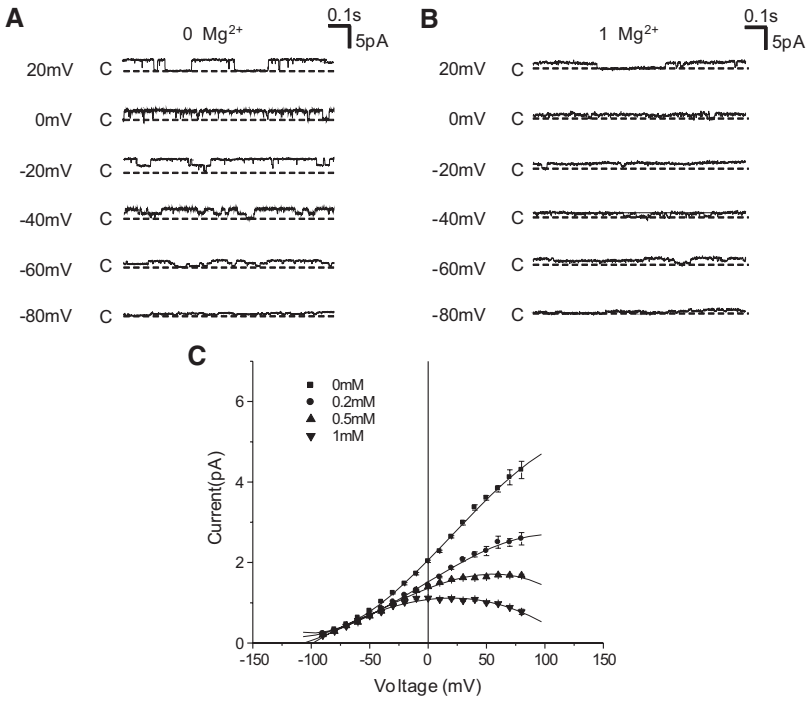

Figure 3. Intracellular Mg^{2+} blocks ROMK currents with 1.1 mM extracellular K^+. (A) Currents in an inside-out patch in the absence of Mg^{2+}. (B) Currents in an inside-out patch in the presence of 1 mM Mg^{2+}. Dashed lines indicate current levels when all channels are closed. (C) *I-V* relationships for 0, 0.2, 0.5, and 1 mM Mg^{2+}. At each voltage, current values represent means ± SEM for 3 to 17 patches. Lines are smooth curves drawn through the points.

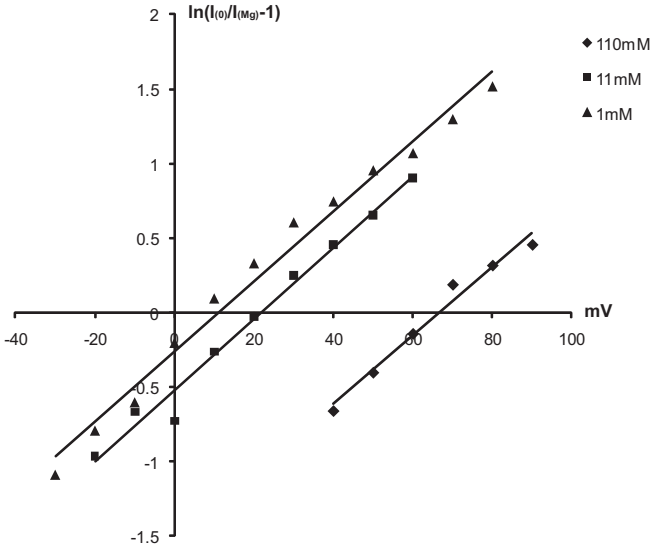

Figure 4. Intracellular Mg^{2+} block depends on membrane voltage. Data from Figures 1 to 3 are replotted as $\ln[(i(0)/i(Mg)) - 1]$ *versus* voltage for 1 mM Mg^{2+}. Straight lines indicate least-square linear regression fits to the equation $y = m \cdot x + b$, where the slope $m = z\delta V/RT$ and the intercept $b = \ln[1/K_i(0)]$ (see equations 1 and 2). Values of the apparent valence of block ($z\delta$) and the apparent K_i at $V = 0$ [$K_i(0)$] obtained from the fits are shown in Table 1.

affinity of Mg^{2+} with decreased external K^+ is also consistent with previous studies.[8] To our knowledge, these are the first measurements of Mg^{2+} block in the range of extracellular K^+ that corresponds to the lowest values observed *in vivo* (*i.e.,* around 1 mM).

Direct recordings from renal cells under conditions of low external K^+ confirmed this effect of internal Mg^{2+} in a more physiologic setting. The TPNQ-sensitive current, indicative of conductance through ROMK channels, was reduced to about 30% of controls by 1.2 mM Mg^{2+} in the absence of a transmembrane voltage (Figure 5). This inhibition is somewhat greater than that measured in excised patches under similar conditions (Figure 2). This could reflect additional Mg^{2+}-dependent processes that downregulate K^+ channels that are lost in excised patches.

In addition to the effects of intracellular ions, ROMK channels were blocked by millimolar concentrations of extracellular Mg^{2+}. A similar interaction has been observed for Kir2.1 channels.[20] The affinity of this block also increased with decreasing K^+. Its mild voltage dependence suggests a binding site located within the outer aspect of the pore.

In most cells, including renal cells, measurements of intracellular Mg^{2+} range from about 0.3 to 1.0 mM.[18] Mg^{2+} may enter the cell down an electrochemical activity gradient through channels such as TrpM6 and TrpM7.[21] It is less clear how the ion is removed from the cells to maintain the gradient. For Mg^{2+} to have an influence on ROMK channel activity, the effective affinity, determined by both voltage-independent and voltage-dependent processes, would need to be in the millimolar range. In ROMK, this is achieved when luminal K^+ concentrations are low. This would pertain to the DCT and also early portions of the CNT, where luminal [K^+] is reduced by reabsorption in the thick ascending limb of Henle's loop and before significant K^+ secretion has taken place.[15]

The presence of other K^+ channel blockers, such as spermine or other polyamines, could compete with Mg^{2+} for blocking sites and therefore reduce the influence of Mg^{2+} on K^+ transport. However, the affinity of ROMK channels for polyamines is low, with K_i values in the millimolar range, and the affinity of Mg^{2+} relative to polyamines is higher in ROMK than in the strong inward rectifier

Table 1. Block of ROMK by intracellular Mg^{2+}

[K^+] (mM)	$z\delta$	$K_i(0)$ (mM)
110	0.62	4.9
11	0.61	1.7
1.1	0.64	1.4

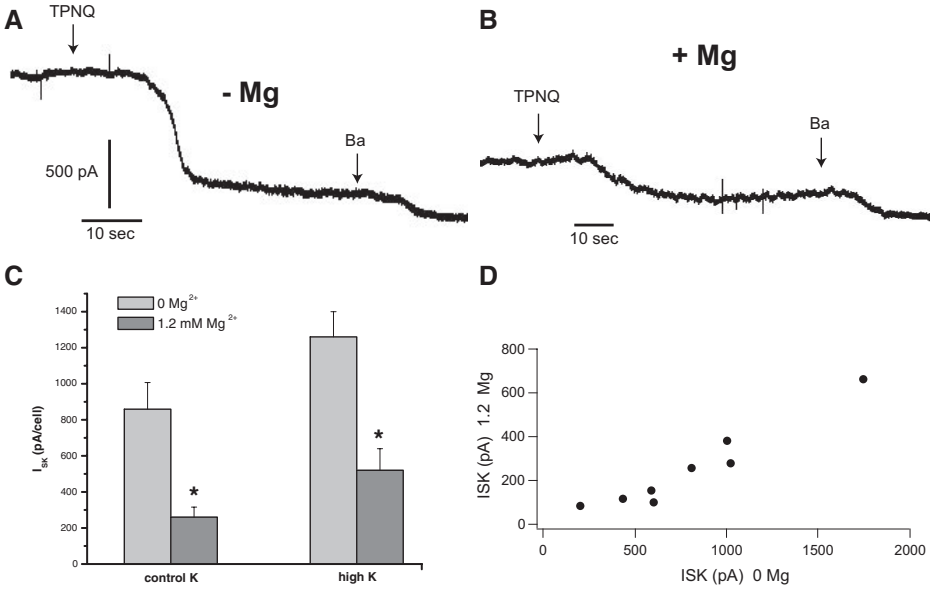

Figure 5. Intracellular Mg^{2+} blocks ROMK currents in principal cells of the rat. (A and B) whole-cell currents from principal cells from the same tubule without (A) or with (B) 1.2 mM Mg^{2+} added to the pipette solution. The voltage was maintained at 0 mV throughout the recordings. Arrows indicate the addition of TPNQ (10^{-7} M) and Ba^{2+} (5 mM) to the bath solution. (C) Mean values of TPNQ-sensitive current (I_{SK}) in the presence and absence of internal Mg^{2+}. Data represent means ± SEM from 13 cells under each condition for animals on a control-K diet. The cells were from eight different tubules obtained from three different rats. Data for the high-K diet represent 26 cells from 4 animals (no Mg) and 13 cells from 2 animals (1.2 mM Mg). (D) Correlation of mean values of I_{SK} in the presence and absence of Mg^{2+} from cells in the same tubules.

Kir2.1.[9] Furthermore, the *I-V* relationship for ROMK in cell-attached patches with high $[K^+]$ on both sides of the membrane can be reasonably well accounted for by Mg^{2+} block with a presumed cytoplasmic concentration of 0.7 mM (Figure 6). These results are consistent with the idea that Mg^{2+} is more important than polyamines in determining the rectification properties of these channels.

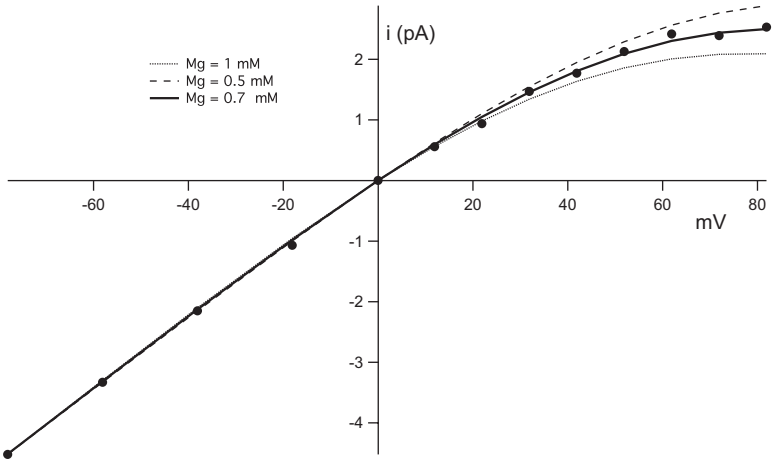

Figure 6. Inward rectification of ROMK currents in the rat CCD is accounted for by intracellular Mg^{2+}. $[K^+]$ in the pipette was 140 mM, approximately equal to the that in the cytoplasm. The solid line represents the predicted currents assuming K_i = 4.9 mM and $z\delta$ = 0.62 as in Figure 4 and intracellular $[Mg^{2+}]$ = 0.7 mM. Upper and lower lines are currents predicted for the same conditions but with $[Mg^{2+}]$ = 0.5 and 1 mM, respectively. Data are from reference 19.

These effects of Mg^{2+} with both the inner and outer parts of the channel are of sufficient magnitude to modulate K^+ secretion under physiologic conditions. One important effect could be to reduce ROMK conductance by Mg^{2+} block, helping to conserve K^+ in K deficiency. Lowering luminal K^+ concentrations through K^+ reabsorption will increase the affinity for Mg^{2+} block from both the lumen and the cytoplasm, lowering rates of K^+ secretion. Our results showed that this mechanism can occur over physiologic concentrations of the ions. Micropuncture studies of rats on a low-K diet indicated that K^+ in the tubular fluid of the distal nephron is maintained at concentrations of 1 to 2 mM.[15] Under these conditions, the K_i for block by cytoplasmic Mg^{2+} is on the order of 1 mM, similar to measured concentrations of 0.5 to 1 mM in renal cells.[22–24] Thus, Mg^{2+} will have a significant inhibitory effect on K^+ secretion under conditions where urinary K^+ loss would be detrimental. This could be particularly useful when the epithelial Na^+ transport rate is high and the luminal membrane is depolarized, increasing the driving force for K^+ secretion but also increasing the affinity for Mg^{2+} block. However, once K^+ in the lumen increases above 10 mM, as occurs under normal or high-K diets,[15] the

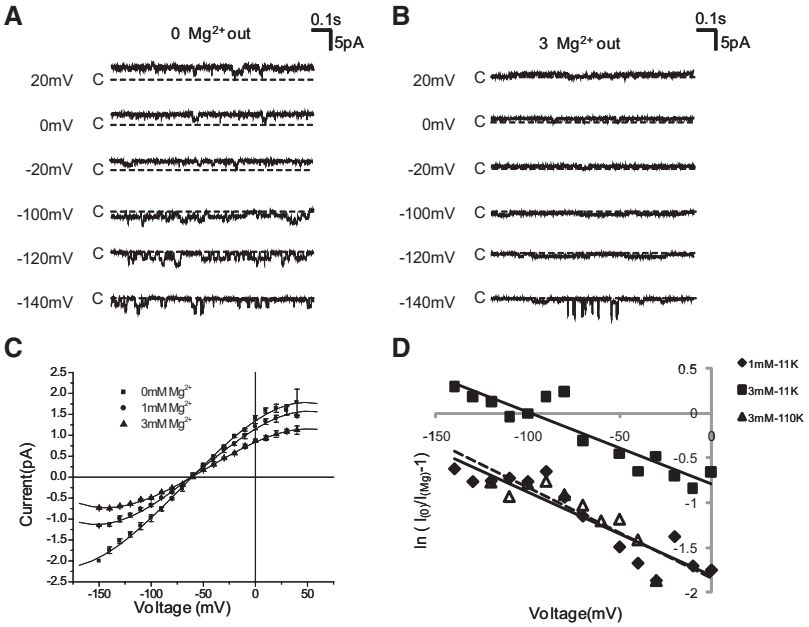

Figure 7. Extracellular Mg^{2+} blocks ROMK currents with 11 mM extracellular K^+. (A) Currents in a cell-attached in the absence of Mg^{2+}. (B) Currents in a cell-attached patch in the presence of 3 mM Mg^{2+}. Dashed lines indicate current levels when all channels are closed. (C) *I-V* relationships for 0, 1, and 3 mM Mg^{2+}. At each voltage, current values represent means ± SEM for two to eight patches. Lines are smooth curves drawn through the points. (D) Data from C are replotted as $\ln[(i(0)/i(Mg)) - 1]$ *versus* voltage. Also plotted are similar results obtained with 3 mM Mg^{2+} and 11 mM extracellular K^+. Straight lines indicate least-square linear regression fits to the equation $y = m \cdot x + b$, where the slope $m = z\delta V/RT$ and the intercept $b = \ln[1/K_i(0)]$ (see equation 1). Estimates of $z\delta$ and $K_i(0)$ obtained from the fits are shown in Table 2.

Mg^{2+} effect will be diminished. Clearly other mechanisms such as the regulation of the number of channels in the apical membrane will affect K^+ secretion during changes in K intake. However, a recent study[16] indicated that a significant ROMK conductance persists even with very low K intake. Thus, under these conditions, inhibition by Mg^{2+} could contribute to K^+ homeostasis by limiting K losses through the channels.

Furthermore, relief of Mg^{2+} block could contribute to K^+ wasting observed during Mg deficiency.[5] Under these conditions, plasma Mg^{2+} concentrations may fall to one third of normal values.[1–3] In cells in culture, cytoplasmic Mg^{2+} decreases in parallel with that in the extracellular medium.[22] Using these values, we can calculate that, for an apical membrane potential around −40 mV and a luminal K^+ of 1 mM, a decrease in cytoplasmic Mg^{2+} from 1 to 0.5 mM would increase K^+ conductance by about 30% (Figure 3C). In addition, Mg^{2+} will be freely filtered by the kidney and will be maintained in the luminal fluid at values close to those of plasma up to the K-secreting portion of the nephron. A decrease in luminal Mg^{2+} from 2 to 1 mM would also increase ROMK conductance by about 10 to 20% (Figure 7C). These effects are not large, but could contribute to K wasting over time. Again, because of the voltage dependence of the effect of intracellular Mg^{2+}, the impact of reduced Mg^{2+} will be largest when the apical membrane voltage is depolarized. This would happen when Na^+ channel activity is elevated as a consequence of volume depletion. This circumstance would apply, for example, to the case of diuretic therapy, a common cause of hypokalemia that is exacerbated by Mg^{2+} deficits.[5] The quantitative significance for such a mechanism under these circumstances is still speculative because we do not know the exact extent of the fall of cytoplasmic Mg^{2+} in renal cells during Mg depletion *in vivo*.

Table 2. Block of ROMK by extracellular Mg^{2+}

$[K^+]_o$ (mM)	$[Mg^{2+}]_o$ (mM)	$z\delta$	$K_i(0)$ (mM)
110	3	0.26	19
11	1	0.24	6.2
11	3	0.20	6.6

CONCISE METHODS

Expression of ROMK2 in Oocytes

pSport plasmids containing rat ROMK2 cDNA were linearized with NotI restriction enzymes (New England Biolabs); cRNAs were transcribed with T7 RNA polymerase using the mMESSAGE mMACHINE kit (Ambion). cRNA pellets were dissolved in nuclease-free water and stored in −70°C before use. Oocytes were harvested from *Xenopus laevis*. All animal protocols were approved by the Institutional Animal Use and Care Committee of Weill-Cornell Medical College. Pieces of ovary were incubated in oocyte Ringer's solution with 2 mg/ml collagenase type II (Worthington) and 2 mg/ml hyaluronidase type II (Sigma-Aldrich) with gentle shaking for 60 minutes and another 30 minutes (if necessary) in a fresh enzyme solution at room temperature. Before injection, oocytes were incubated in oocyte Ringer's solution for 2 h at 19°C. Defolliculated oocytes were selected and injected with 0.15 to 0.5 ng cRNA. They were stored at 17°C for 24 to 48 hours in modified Barth's solution containing (in mM) 85 NaCl, 1 KCl, 0.7 $CaCl_2$, 0.8 $MgSO_4$, and 5 Hepes, pH 7.4, to permit channel expression. All chemicals were from Sigma-Aldrich unless otherwise noted.

Patch Clamp

Before use, the vitelline membranes of the oocytes were mechanically removed in a hypertonic solution containing 200 mM sucrose. Patch-clamp pipettes were prepared from hematocrit capillary glass (VWR Scientific) using a vertical puller (Kopf Instruments). They were used without fire-polishing and had resistances of 2 to 8 MΩ. Pipette solutions contained (in mM) 110 KCl and 5 Hepes, pH 7.4, or reduced KCl (11 or 1 mM) with substitution by NaCl (99 or 109 mM). Bath solutions contained (in mM) 110 KCl, 0.2 to 3 mM $MgCl_2$ or 0.1 mM $BaCl_2$, 0.5 mM EGTA and 5 Hepes, at pH 7.4. Currents from cell-attached and excised inside-out patches were recorded with an EPC-7

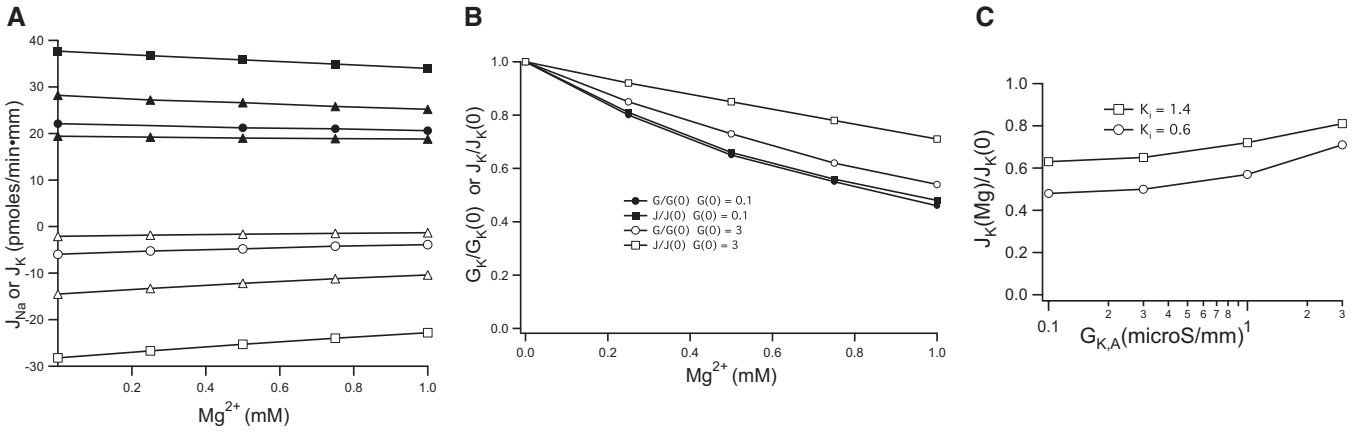

Figure 8. Intra- and extracellular Mg^{2+} reduce K^+ secretion in a numerical model of the rat CNT. (A) The effects of Mg^{2+} on absorptive ($J_{Na} > 0$) Na fluxes (solid symbols) and secretory ($J_K < 0$) K fluxes (open symbols) were calculated for four different values of the unblocked apical K^+ conductance (G_{KA} = 3, 1, 0.3, and 0.1 μS/mm). (B) The ratio of J_K values with 1 and 0 mM Mg^{2+} are plotted at different G_{KA}. (C) The relative decreases in G_{KA} and J_K with increasing Mg^{2+} at G_{KA} = 3 and 0.1. Values of the apical membrane voltage were −53 to −61 mV for G_{KA} = 3 and −32 to −34 mV for G_{KA} = 0.1.

patch-clamp amplifier (Heka Elektronik) for 10 minutes and digitized with a Digidata 1332A interface (Axon Instruments). Data were filtered at 0.5 kHz and analyzed with pCLAMP9 software (Axon Instruments). Single-channel current amplitudes were measured from individual current transitions using pCLAMP 9 software.

Block by Mg^{2+} and other ions was analyzed according to the equations:

$$i(\mathrm{Mg}) = i(0)/(1 + [\mathrm{Mg}^{2+}]/K_{\mathrm{i,Mg}}) \quad (1)$$

$$K_{\mathrm{i,Mg}}(V) = K_{\mathrm{i,Mg}}(0)\exp(-zF\delta V/RT)$$

where i is the single-channel current at a given concentration of Mg^{2+} and voltage (V), and $K_{i,Mg}$ is the apparent K_i that is also a function of voltage. The apparent valence of the blocking reaction is given by $z\delta$. For the simplest type of voltage-dependent block, z is the charge (+2) on the blocking ion, and δ is the fraction of the transmembrane electric field crossed by the blocker to reach its blocking site. These equations can be linearized by plotting $\ln[i(0)/i(\mathrm{Mg}) - 1]$ *versus* V. The slopes of these plots indicate the effective valence $z\delta$ and the intercepts K_i in the absence of a membrane voltage.

CCD Recordings

CCDs were isolated from the kidneys of female Sprague-Dawley rats (200 to 250 g) raised free of viral infections (Charles River Laboratories, Kingston, NY) and fed a standard rodent chow. A group of rats was fed a 10% KCl–containing diet (Harlan-Teklad, Madison, WI) for 1 week to increase K intake. Measurement of whole-cell K^+ currents in principal cells of the CCD followed procedures described previously.[16,25] Split-open tubules were superfused with solutions prewarmed to 37°C containing (in mM) 135 Na methanesulfonate, 5 KCl, 2 Ca methanesulfonate, 1 $MgCl_2$, 2 glucose, and 10 Hepes, adjusted to pH 7.4 with NaOH. The patch-clamp pipettes were filled with solutions containing (in mM) 7 KCl, 123 aspartic acid, 5 EGTA, and 10 Hepes, with the pH adjusted to 7.4 with KOH. Where indicated, 1.2 mM Mg gluconate was added to the pipette solution. The free Mg^{2+} concentration was estimated to be 1.1 mM. The total concentration of K^+ was approximately 145 mM. TPNQ (Sigma-Aldrich, St. Louis, MO) was dissolved in H_2O at a concentration of 100 μM and diluted into the bath solution to final concentration of 100 nM. Ba acetate was added to the bath solution to a final concentration of 5 mM. Pipettes were pulled from hematocrit tubing, coated with Sylgard, and fire polished with a microforge. Pipette resistances ranged from 2 to 5 MΩ. Voltages were controlled and currents recorded using an ITC-16 interface (Instrutech, Mineola, NY) and Pulse software (HEKA).

A numeric model of Na and K transport in the CCD/CNT was used as described previously.[16,19] The basic model parameters were those previously used to describe the CNT with moderate Na transport rates: apical Na permeability = 1.8×10^{-8} cm^3/s·mm tubule; basolateral K conductance = 7.7 μS/mm tubule; paracellular permeability = 1 μS/mm tubule; luminal $[Na^+]$ = 30 mM; and luminal $[K^+]$ = 5 mM. The apical K conductance was varied from 0.1 to 3 μS/mm.

ACKNOWLEDGMENT

This work was supported by National Institutes of Health Grant RO1-DK27847.

DISCLOSURES

None.

REFERENCES

1. Francisco LL, Sawin LL, Dibona GF: Mechanism of negative potassium balance in the magnesium-deficient rat. *Proc Soc Exp Biol Med* 168: 382–388, 1981
2. Whang R, Welt LG: Observations in experimental magnesium depletion. *J Clin Invest* 42: 305–313, 1963

3. Wong NL, Sutton RA, Mavichak V, Quamme GA, Dirks JH: Enhanced distal absorption of potassium by magnesium-deficient rats. *Clin Sci (Lond)* 69: 625–630, 1985
4. Solomon R: The relationship between disorders of K^+ and Mg^{2+} homeostasis. *Semin Nephrol* 7: 253–262, 1987
5. Huang CL, Kuo E: Mechanism of hypokalemia in magnesium deficiency. *J Am Soc Nephrol* 18: 2649–2652, 2007
6. Matsuda H, Saigusa A, Irisawa H: Ohmic conductance through the inwardly rectifying K channel and blocking by internal Mg^{2+}. *Nature (Lond)* 325: 156–159, 1987
7. Vandenberg CA: Inward rectification of a potassium channel in cardiac ventricular cells depends on internal magnesium ions. *Proc Natl Acad Sci USA* 84: 2560–2564, 1987
8. Lu Z, MacKinnon R: Electrostatic tuning of Mg^{2+} affinity in an inward-rectifier K^+ channel. *Nature* 371: 243–246, 1994
9. Taglialatela M, Ficker E, Wible BA, Brown AM: C-terminus determinants for Mg^{2+} and polyamine block of the inward rectifier K^+ channel IRK1. *EMBO J* 14: 5532–5541, 1995
10. Yang J, Jan YN, Jan LY: Control of rectification and permeation in residues in two distinct domains in an inward rectifier K^+ channel. *Neuron* 14: 1047–1054, 1995
11. Ishihara K, Yan DH: Low-affinity spermine block mediating outward currents through Kir2.1 and Kir2.2 inward rectifier potassium channels. *J Physiol* 583: 891–908, 2007
12. Leech CA, Stanfield PR: Inward rectification in frog skeletal muscle fibres and its dependence on membrane potential and external potassium. *J Physiol (Lond)* 319: 295–309, 1981
13. Lopatin AN, Nichols CG: $[K^+]$ dependence of polyamine-induced rectification in inward rectifier potassium channels (IRK1, Kir2.1). *J Gen Physiol* 108: 105–113, 1996
14. Chepilko S, Zhou H, Sackin H, Palmer LG: Permeation and gating properties of a cloned renal K^+ channel. *Am J Physiol* 268: C389–C401, 1995
15. Malnic G, Klose R, Giebisch G: Micropuncture study of renal potassium excretion in the rat. *Am J Physiol* 206: 674–686, 1964
16. Frindt G, Shah A, Edvinsson JM, Palmer LG: Dietary K regulates ROMK channels in connecting tubule and cortical collecting duct of rat kidney. *Am J Physiol* 296: F347–F354, 2009
17. Carney SL, Wong NL, Quamme GA, Dirks JH: Effect of magnesium deficiency on renal magnesium and calcium transport in the rat. *J Clin Invest* 65: 180–188, 1980
18. Quamme, GA: Magnesium: Cellular and renal exchanges. In: *The Kidney: Physiology and Pathopohysiology*, 2nd Ed., edited by Seldin DW, Giebisch G, New York, Raven Press, 1992, pp 2339–2355
19. Gray DA, Frindt G, Palmer LG: Quantification of K^+ secretion through apical low-conductance K channels in the CCD. *Am J Physiol Renal Physiol* 289: F117–F126, 2005
20. Murata Y, Fujiwara Y, Kubo, Y: Identification of a site involved in the block by extracellular Mg^{2+} and Ba^{2+} as well as permeation of K^+ in the Kir2.1 K^+ channel. *J Physiol* 554: 665–677, 2002
21. Alexander RT, Hoenderop JG, Bindels RJ: Molecular determinants of magnesium homeostasis: Insights from human disease. *J Am Soc Nephrol* 19: 1451–1458, 2008
22. Dai LJ, Raymond L, Friedman PA, Quamme GA: Mechanism of amiloride stimulation of Mg^{2+} uptake in immortalized mouse distal convoluted tubule cells. *Am J Physiol* 272: F249–F256, 1997
23. Ikari A, Atomi K, Kinjo K, Sasaki Y, Sugatani, J: Magnesium deprivation inhibits a MEK-ERK cascade and cell proliferation in renal epithelial Madin-Darby canine kidney cells. *Life Sci* 86: 766–773, 2010
24. Ikari A, Nakajima K, Suketa Y, Harada H, Takagi K: Arachidonic acid-activated Na^+-dependent Mg^{2+} efflux in rat renal epithelial cells. *Biochim Biophys Acta* 1618: 1–7, 2003
25. Gray DA, Frindt G, Zhang YY, Palmer LG: Basolateral K^+ conductance in principal cells of rat CCD. *Am J Physiol Renal Physiol* 288: F493–F504, 2005